

A Chaotic Associative Memory

N. Rajagopal Rohan,^{1,2} Sayan Gupta,^{2,3} and V. S. Chakravarthy^{1,3}

¹Laboratory of Computational Neuroscience, Bhupat and Jyoti Mehta School of Biosciences and Biotechnology, Indian Institute of Technology Madras, Chennai - 600036, India

²The Uncertainty Lab, Department of Applied Mechanics, Indian Institute of Technology Madras, Chennai - 600036, India

³Center for Complex Systems and Dynamics, Indian Institute of Technology Madras, Chennai - 600036, India

(*Electronic mail: schakra@ee.iitm.ac.in)

(*Electronic mail: sayan@iitm.ac.in)

(Dated: 23 January 2024)

We propose a novel Chaotic Associative Memory model using a network of chaotic Rossler systems and investigate the storage capacity and retrieval capabilities of this model as a function of increasing periodicity and chaos. In early models of associative memory networks, memories were modeled as fixed points, which may be mathematically convenient but has poor neurobiological plausibility. Since brain dynamics is inherently oscillatory, attempts have been made to construct associative memories using nonlinear oscillatory networks. However, oscillatory associative memories are plagued by the problem of poor storage capacity, though efforts have been made to improve capacity by adding higher order oscillatory modes. The chaotic associative memory proposed here exploits the continuous spectrum of chaotic elements and has higher storage capacity than previously described oscillatory associative memories.

In indexed memories used in a computer, the right address has to be known to fetch the corresponding content. Contrasting, in a human or an associative memory, there is no division between the "address" and the "content": a part of the content can itself serve as an "address." Thus when the system is cued by an incomplete pattern it retrieves the corresponding complete pattern. In early network models of associative memories, memories were stored as fixed points. Subsequently, in recognition of the incessant oscillatory activity of the brain, oscillatory associative memories have been proposed. However, oscillatory associative memories suffer from the problem of poor storage capacity. Here we describe a chaotic associative memory in which memories are stored as chaotic attractors. The model has higher storage capacity than the previously described oscillatory associative memories. The model is also justified by experimental studies in literature that showed that memories of odors are stored as chaotic attractors in the olfactory bulb.

items. For example when we think of the city of Paris we think of the Eiffel tower and vice versa. There is no separate "address" and "content". Depending on the context, Paris can be the address (content) and Eiffel toward can be the content (address). Referring to this lack of distinction between the address and the content, associative memories are sometimes referred to as Content Addressable Memories.

One of the earliest of such models, proposed by Hopfield², consisted of a network of sigmoid neurons with binary states, in which memories are stored using Hebb's rule². This mode was subsequently extended to continuous states and continuous time³. The aforementioned models serve as pattern-completion systems in which the network takes an incomplete pattern as input and retrieves the corresponding complete pattern i.e., the networks are unidirectional. Kosko⁴ generalized such networks to bidirectional associative memories in which there are separate input and output channels, an idea further extended to multidimensional associative memories. The Boltzmann machine is an extension of these models in which there are hidden or invisible neurons in addition to the input/output neurons⁵.

I. INTRODUCTION

The idea that attractors of neural dynamics can be interpreted as memories in the brain had paved the way to an important class of memory models - the neural associative memories¹. An associative memory is a type of memory that is akin to human memory. In contrast to the human memory, a computer memory, which is sometimes described as an indexed memory, is organized as a long of addresses and the corresponding contents. If we wish to retrieve a certain content, we must know the corresponding address like, for example, the call number of a book in a library. In a human memory, on the other hand, there is no separate address and the content. We often store information as a network of items from which items are recalled by associating them with other

The working principle of the models discussed above become apparent when viewed as dynamical systems. These models have certain common features - existence of a Lyapunov or an "energy" function, retrieval dynamics depends on performing gradient descent on the Lyapunov function and memories are therefore local minima of the Lyapunov function, or fixed points of the retrieval dynamics. Hence, the efficacy of any associative memory model is a measure of increasing stability of the fixed points associated to the stored memories. Stability analysis in a more general class of associative memory networks were studied by Cohen and Grossberg⁶.

Brain is a dynamic environment and memories do not seem to be encoded as fixed points in brain dynamics. There is evidence that memories are encoded in terms of neural oscillations, particularly in the theta (4 - 8 Hz) and gamma (30 - 80 Hz) bands^{7,8}. Memories related to spatial locations⁹ and objects¹⁰ were found to be encoded as neural oscillations. Associative memory models in which memories are stored as oscillatory states have been proposed. Abbot¹¹ proposed an oscillatory neural network in which binary vectors are stored as phase relationships among neural oscillations. Generalizing the continuous-state Hopfield network³ to complex-variable domain, Chakravarthy and Ghosh¹² proposed an oscillatory associative memory in which memories are oscillatory states. Oscillatory memories have a particular appeal from the point of view of hardware realizations e.g. in the form of laser oscillations¹³ or MEMS resonators¹⁴.

Despite their obvious biological appeal, oscillatory memories suffer from serious limitations in storage capacity. It turns out that, irrespective of the network size, oscillatory networks are typically unstable when the number of stored memories exceeds 2¹⁵. To overcome this serious limitation Nishikawa et al¹⁶ had proposed an additional oscillatory term corresponding to second-order mode, thereby achieving a nontrivial storage capacity of $\frac{2n\epsilon^2}{\ln(n)}$, where n is the number of oscillator neurons and ϵ is the strength of second order coupling. Going further on the same lines Follman et al¹⁷ had proposed an oscillator network in which further improvements in storage capacity and retrieval accuracy was obtained by adding a third order mode to oscillator dynamics. While previous studies have demonstrated that models of oscillatory memories with a single native frequency suffer from limitations of capacity, that this problem can be somewhat alleviated by including higher modes this seems to indicate that the storage capacity can be improved by expanding the spectral bandwidth of the memory model.

In their pioneering studies of odor memories in the olfactory bulb, Freeman and colleagues¹⁸ have shown that odors are stored as elements of weakly chaotic attractors. They propose that chaos acts as a controlled deterministic source of noise. In a network of neurons dedicated to sensory processing, such noise is thought to drive a continual access to previously learned sensory pattern and to possibly learn new sensory information¹⁸. Further, they conjectured that chaotic activity provides a way of exercising neurons that is guaranteed not to lead to cyclic entrapment and to allow impartial access to all the stored odours. The Chaotic Associative Memory (CAM) model proposed in this paper is inspired by the ideas of Freeman and molds it as a natural extension to the existing methodologies to overcome the capacity limitation of Oscillatory Associative Memory (OAM) models. We use the well-known Rossler system as the fundamental unit or neuron. The power spectrum of a continuous dynamical system in the chaotic regime of period doubling due to phase modulation and amplitude modulation broadens¹⁹, i.e. as the Rossler system transitions to chaos, broad spectral components are added

to the power spectral density. We leverage these characteristics to propose a natural improvement to the OAM and improve the ability to retrieve the stored memories.

In Sec. II that follows, we introduce certain elements of Hopfield Networks and the current OAM models that can pave the way to construct CAM. The CAM model and relevant definitions are introduced in Sec. III, while Sec. IV presents the results and analysis. In the final section, Sec V, we note the salient features of our model, specifically in translating the ideas of Freeman and coworkers, and compare it with advancements of a similar nature.

II. PREREQUISITES TO THE CAM MODEL

A. The Hopfield Network

The Hopfield Neural Network is a network of neurons topologically arranged as a completely connected weighted graph, where the weights corresponding to the edges represent the strength of "association" between neurons. A network of N Hopfield neurons has an internal state, v_i , that takes values ± 1 only, and the interactions are governed by a weight matrix, denoted as \mathbf{W} , learned by Hebb's law of association. The evolution of the Hopfield neurons is described by the following update rule,

$$v_i(t+1) = \sigma\left(\sum_{j=1}^N W_{ij}v_j(t)\right) \quad (1)$$

where $\sigma(x) = \tanh(x)$. A pattern is represented as a vector $(b_1^{(\eta)} \dots b_N^{(\eta)})$, $b_i^{(\eta)} = \pm 1$ and $\eta = 1, \dots, p$. The associated weight matrix W for a set of p patterns is given by

$$W_{ij} = \sum_{\eta=1}^p b_i^{(\eta)} b_j^{(\eta)}. \quad (2)$$

As the weights are obtained as dot product of a pattern with itself, \mathbf{W} takes integer values not greater than p . Given a new pattern at $t = 0$, the Hopfield network evolves to a stored pattern that is nearest to the stimulating pattern.

B. Oscillatory Associative Memory Models

The oscillatory associative models are based on phase oscillators, most commonly on Kuramoto type oscillators, where the patterns are stored as functions of anti - phase synchronisations. The dynamics of each neuron of a network of N phase oscillators can be expressed as:

$$\begin{aligned} \dot{\theta}_i = & \omega_i + \epsilon \sum_{j=1}^N W_{ij} \sin(\theta_j - \theta_i) \\ & + \sum_{k=2}^{K \subseteq N} \left(\frac{\epsilon_k}{N} \sum_{j=1}^N W_{ij} \sin k(\theta_j - \theta_i) \right) \\ & i = 1, \dots, N \end{aligned} \quad (3)$$

where \mathbf{W} is the weight matrix as defined in Eq(2), and K represents the number of Fourier modes added for increased retrieval performance as mentioned in Sec. I. Here the patterns are encoded as locked (or steady state) phase deviations of the oscillators. We note here that Eq. (3) is translational invariant, i.e. for any solution $\theta(t)$ of Eq.(3) and $\mathbf{c} \in \mathbb{R}^N$, $\theta(t) + \mathbf{c}$ is also a solution.

The system defined by Eq.(3) has 2^N fixed points corresponding to all the binary patterns of length N . Given a pattern $(b_1^{(\eta)} \cdots b_N^{(\eta)})$, there is a unique (up to constant translation) fixed point solution that corresponds to the pattern as described below,

$$|\theta_i - \theta_j| \approx \begin{cases} 0, & \text{if } b_i = b_j, \\ \pi, & \text{if } b_i \neq b_j. \end{cases} \quad (4)$$

C. Rossler System

For our Chaotic Associative Memory model we employ the well studied Rossler system,

$$\begin{aligned} \dot{x} &= -\omega y - z, \\ \dot{y} &= \omega x + \alpha y, \\ \dot{z} &= f + z(x - \mathbf{c}). \end{aligned} \quad (5)$$

where (α, f, \mathbf{c}) are the parameters of the Rossler system and ω refers to the angular velocity. For the parameters $\alpha, f = 0.1$ and \mathbf{c} is increased in the range $[4, 14]$, the system undergoes a series period doubling bifurcations, ultimately exhibiting chaotic behaviour, as shown in Fig. 4A; with increasing chaos the frequency spectrum becomes richer and the spectral bandwidth increases.

III. CHAOTIC ASSOCIATIVE MEMORY (CAM) MODEL

To develop an associative memory model for the Rossler system inspired by the phase oscillator model, we need to introduce corresponding terms. As described in²⁰ for the Rossler system, it is advantageous to transform the phase and amplitude to the polar coordinate form by introducing the variables

$$\phi = \tan^{-1}(y/x), \quad A = (x^2 + y^2)^{1/2}. \quad (6)$$

We rewrite Eq.(5),

The Chaotic Associative Memory model is a network of N Rossler systems or neurons, arranged in a similar topology to the Hopfield Network. The dynamics of each individual CAM neuron, defined by Eq (6), is given by

$$\begin{aligned} \dot{A}_i &= (\alpha A_i \sin^2 \phi_i - z_i \cos \phi_i) + \varepsilon \left(\sum_{j=1}^N W_{ij} \cos(\phi_j - \phi_i) \right), \\ \dot{\phi}_i &= (\omega + \alpha \sin \phi \cos \phi + z/A \sin \phi), \\ &\quad + \varepsilon \left(\sum_{j=1}^N W_{ij} \sin(\phi_j - \phi_i) \right) \\ z_i &= f - \mathbf{c} z_i + A_i z_i \cos \phi_i. \end{aligned} \quad (7)$$

where the weight matrix W is defined by Eq(2). \mathbf{c} is the parameter that we use to control the period doubling bifurcation to chaos as stated in Sec II-C. The model is a network of weakly coupled chaotic system, that is the coupling strength ε is $\mathcal{O}(10^{-3})$. Given a set of initial conditions, the model evolves to a pattern that is closest to the stimulating external input.

A. Energy Function

We propose that the energy (Lyapunov type) function of the system can be approximated as,

$$\mathcal{L}(\phi; \mathbf{W}, \varepsilon) = -\Re \left(\sum_{i,j=1}^N W_{i,j} e^{i\phi_i} e^{-i\phi_j} \right). \quad (8)$$

We reason this by the following argument: If we introduce the slow phase θ_i as $\phi_i = \omega_i t + \theta_i$, and average the equations as demonstrated in²⁰ then the system reduces to the Lyapunov function of an **OAM** operating in single Fourier mode (defined by Eq.(3) but without the second summation term) which can be written as

$$\mathcal{L}(\theta; \mathbf{W}, \varepsilon) = -\Re \left(\sum_{i,j=1}^N W_{i,j} e^{i\theta_i} e^{-i\theta_j} \right). \quad (9)$$

Combining Eqs (2) and (9), the energy per oscillator can be written as

$$\overline{\mathcal{L}}(\phi; \mathbf{W}, \varepsilon) = \frac{1}{N} \mathcal{L}(\phi; \mathbf{W}, \varepsilon) = -\frac{1}{2} \sum_{\eta=1}^p m_{\eta}^2, \quad (10)$$

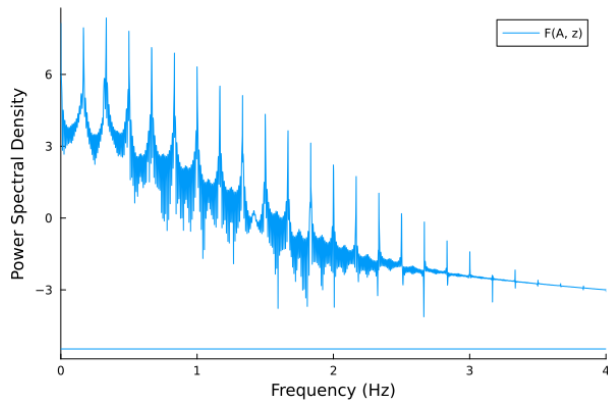
where $m_{\eta} = m_{\eta}(\phi) = \left| \frac{1}{N} \sum_{j=1}^N b_j^{(\eta)} e^{i\phi_j} \right|$, $\eta = 1 \cdots p$. The parameter m_{η} is called the overlap parameter, and is a measure of the closeness of the solution to the binary pattern $b^{(\eta)}$. As noted in¹⁶, the minimum of Eq. (10) is typically near but off the fixed point corresponding to one of the patterns m_{η} . We conjecture that the phase deviations caused by the state variable z_i term possibly help stabilize the system for greater retrieval performance as shown in the following section. We briefly elaborate on this in Sec-III B. The existence of this energy function $\mathcal{L}(\phi; \mathbf{W}, \varepsilon)$ as stated in Eq.(9) ensures that any solution of the system converges to a phase-locked solution as $t \rightarrow \infty$.

B. The Role of Dynamical Noise

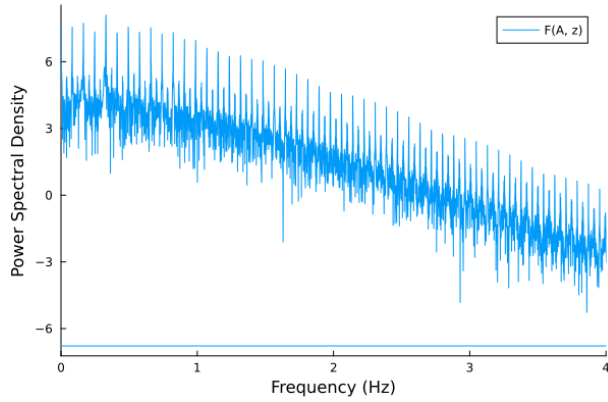
We can represent the time evolution of ϕ , the phase variable for a chaotic oscillators, as follows²⁰⁻²²,

$$\dot{\phi} = \omega + F(A) \quad (11)$$

where, ω represents the mean angular frequency of the oscillations, and the term $F(A)$ represents the amplitude dependence of the frequency and in general is assumed to be



(a) figure

PSD of $F(A, z)$ in logarithmic scale for $c = 4$ 

(b) figure

PSD of $F(A, z)$ in logarithmic scale for $c = 9$

FIG. 1: The power spectral density plots show the addition of harmonics to the phase dynamics of the CAM model.

chaotic. This can be generalised to represent the phase variable of Eq.(8) as

$$\dot{\phi}_i = \omega + F(A_i, z_i) + \varepsilon \left(\sum_{j=1}^N W_{ij} \sin(\phi_j - \phi_i) \right), \quad (12)$$

where

$$F(A, z) = a \sin \phi \cos \phi + z/A \sin \phi. \quad (13)$$

In this representation, the $F(A, z)$ constitutes the dynamical noise term. The power spectral density (PSD) plots of $F(A, z)$ in the periodic regime is shown in Fig.1(a) and corresponding figure for the sparse chaotic regime is shown in Fig.1(b).

From Fig.1 it can be seen that there exist a larger number of harmonics. This in turn is equivalent to the addition of a larger number of harmonic terms in the context of previous studies to enhance the stability of oscillator based associative memory model^{16,17}. As expected in the sparse chaotic regime the power spectral density is almost like a continuum, allowing for greater retrieval performance of the proposed model (as will be shown later in this paper).

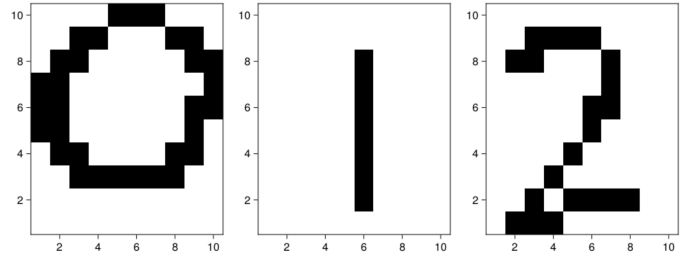
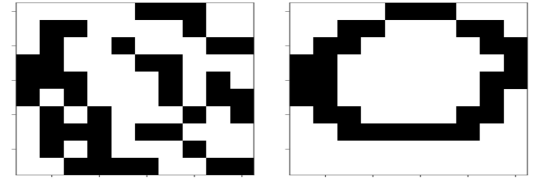
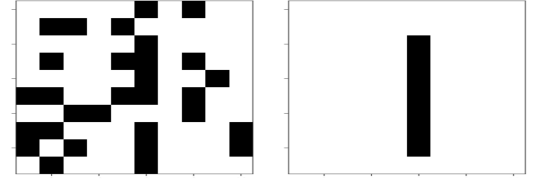


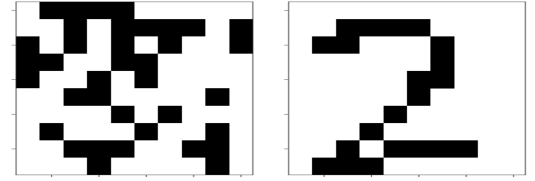
FIG. 2: The patterns stored in the CAM Model.



(a) For Pattern 0



(b) For Pattern 1



(c) For Pattern 2

FIG. 3: Left column: noisy patterns introduced as initial states, Right column: corresponding final retrieved pattern

IV. NUMERICAL ANALYSIS AND RESULTS

The CAM model was implemented in Julia²³, using the SciML libraries DifferentialEquations.jl²⁴, ModelingToolkit.jl²⁵, and Sundial.jl^{26,27}. The system of differential equations was solved using various solvers available therein.

We first demonstrate the capabilities of the CAM model by storing the the figures showed in Fig. 2 from the popular MNIST dataset²⁸ for $N = 100$ and $c = 13$, represented in a 10×10 lattice structure by dimensional reduction. We have reduced the dimension of the images for computational efficiency. Each of these patterns are fed to the model with 30% erroneous bits as the initial conditions at $t = 0$. Subsequently the governing equations Eq.(8) are evolved in time for long time duration. Fig. 3 shows the initial pattern introduced to the model and the retrieved pattern, showing complete or perfect retrieval in all cases.

We analyse the effect of increasing c on the retrieval capabilities, as each CAM neuron transitions between periodic, or chaotic regimes, we simulate the model for $N = 100$, for several parameter cases where c . To quantify the accuracy of the patterns retrieved we use the Hamming distance measure for $\mathbf{x}, \mathbf{y} \in \mathbb{R}^N$, $\mathcal{D}(\mathbf{x}, \mathbf{y}) = N - |I|$, where $I := \{i | x_i \approx y_i\}$. We make a modification to this; since our network of chaotic oscillators doesn't exhibit perfect anti-phase synchronisation, we allow for some tolerance when checking for equality. To take into account the effect of different initial conditions and the nature of patterns, for a given value of c , the average Hamming distance is computed using the following algorithm.

Algorithm 1 Average Hamming Distance, $\mathcal{E}\%$ noise

Require: $c \in [4, 14]$, P $\triangleright P$ is the pattern set
 $i \leftarrow 0$,
 $sum_d_2 = 0$
while $i \leq |P|$, **do**
 $\mathbf{x} \leftarrow \mathbf{b}^{(i)}$
 $sum_d_1 = 0$
 while $j \leq \mathfrak{K}$ **do** $\triangleright \mathfrak{K}$: calculating the avg.
 $\bar{\mathbf{b}}^{(i)} \leftarrow$ invert polarities of $\mathcal{E}\%$ of $\mathbf{b}^{(i)}$
 $\mathbf{y} \leftarrow CAM(c, \bar{\mathbf{b}}^{(i)})$
 $d_1 \leftarrow \mathcal{D}(\mathbf{x}, \mathbf{y})$
 $sum_d_1 \leftarrow sum_d_1 + d_1$
 end while
 $d_2 \leftarrow \text{mean}(sum_d_1)$
 $sum_d_2 \leftarrow sum_d_2 + d_2$
end while
avg_Hamming_dist = $\text{mean}(sum_d_2)$
return avg_Hamming_dist

We note here that each $\mathbf{b}^{(\eta)}$ is chosen randomly and independently to be ± 1 with equal probability for a pattern set.

The variation of the averaged Hamming distance measure as a function of parameter value c is shown in Fig. 4(C), where the average Hamming distance is calculated as per **Algorithm 1** for 10 different pattern sets P . It is observed that the average Hamming distance show significant dips for specific values of c indicating good recovery of the stored patterns at these values of c . The peaks are marked by the red solid lines, and the valleys are denoted by black dashed lines. The dynamics of the network of Rossler systems evolve in a very high dimensional state space and consequently it is difficult to correlate the trends shown in Fig.4(C) with its dynamics. However, since the CAM model is a set of weakly coupled chaotic Rossler systems, with coupling coefficient ε of $O(10^{-3})$, insights can be obtained by investigating the bifurcation diagram of a single Rossler system. Moreover, as emphasised in Sec-III B, the innate dynamical noise of the Rossler system in each node plays a role in stabilising the stored patterns and suggests a possible relationship with the behaviour of the Model to the dynamical properties of each node.

For the first two valleys, we are unable to make any definite correlation apart from the fact that the maximum Lyapunov exponent are almost zero at these points (indicating periodic behavior). Additionally, the first two minima cor-

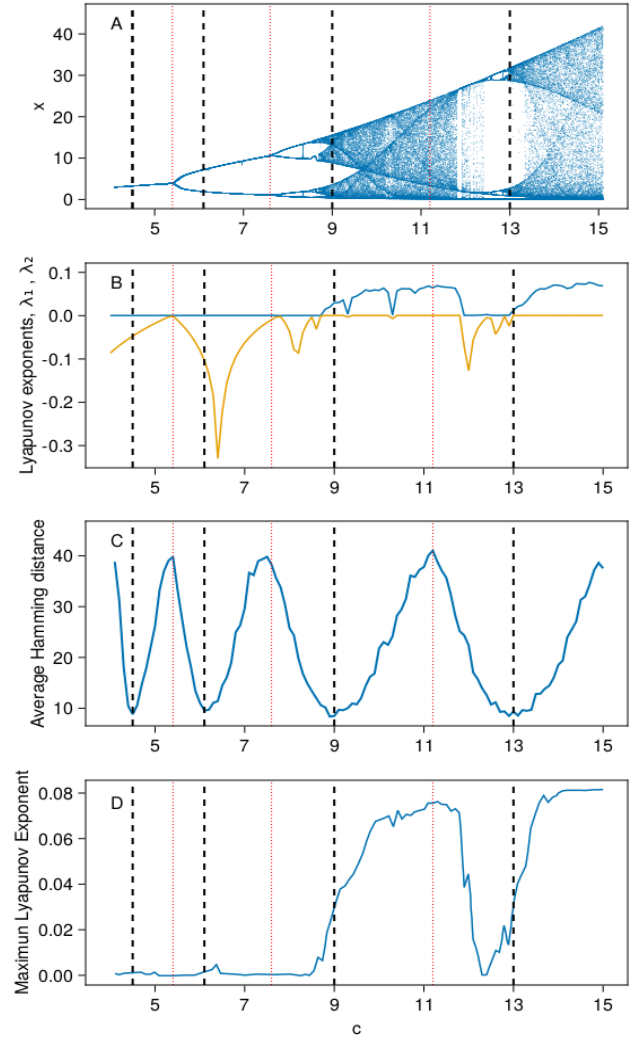


FIG. 4: The dynamical properties of each individual node are characteristic to the properties of the entire system. Drawn along the common axes is the bifurcation parameter c . **A.** The bifurcation diagram of a single Rossler system $a = 0.1, f = 0.1$. The system exhibits period doubling bifurcations, transitioning from periodic orbits to chaotic attractors. **B.** The two largest Lyapunov exponents of a single Rossler node are shown. **C.** The average Hamming distance is shown for $p = 10, N = 100$. **D.** The Maximum Lyapunov exponent (MLE) of the CAM model. The black dashed lines marked μ_i , are the local minima in average Hamming distance calculations, and the red lines are the maxima. The dashed black lines represent the valleys as observed in C. The red lines represent the peaks.

respond to the more stable periodic states as described by $\lambda_2 < 0$ in Fig.4(B). However, we do notice that the third and the fourth valleys appear to be in the neighborhood of critical points where the single Rossler system transitions to chaos; see Fig. 4(B). Further, we observe that the peak at $c \approx 5.5$ corresponds to where a period doubling occurs. The next peak which occurs in between 7 and 9 is in the neighbourhood of

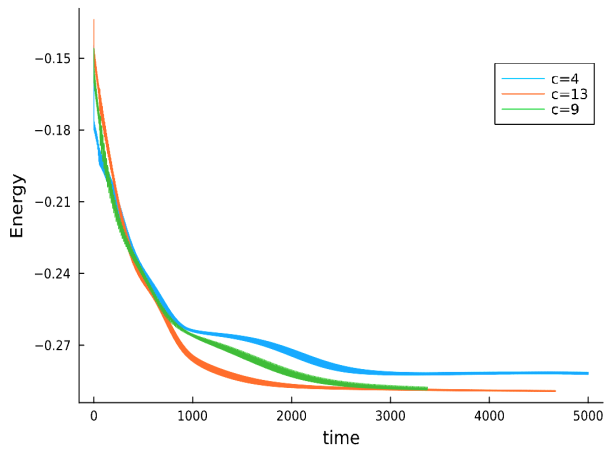


FIG. 5: The three curves represent the energy levels for $c = 4$ (black), $c = 9$, (Green), and $c = 13$, (Red), for $N = 50$, $p = 6$. This shows a greater retrieval ability of CAM system in sparse chaotic regime.

another period doubling observed in a single Rossler system; the slight variation could be on account of the effects of coupling. Additionally, at these points λ_2 increases to 0. However, it is difficult to make any correlation with the third peak and the bifurcation diagram in Fig.4(A). More investigations are necessary to have a clearer understanding of these issues. Fig. 5 shows the effect on the evolution of the proposed energy function with time for $c = 4$, periodic, and 9 and 13, sparse chaotic regimes. We observe that the energy state of the system as described by Eq. (9) in the sparse chaotic regime is lower than that of a single period regime indicating greater retrieval ability. These plots additionally show overall stability of the retrieved pattern.

We next analyse the effect of $c \in [4, 14]$ at certain appropriate values, depending on the performance observed in Fig. 6 and the period doubling bifurcations of a single Rossler system noted in Sec-II C. In Fig. 6 we plot the average Hamming distance as a function of the number of patterns stored. The average Hamming distance is computed using **Algorithm 1** with the initial pattern fed to the model with 20% erroneous bits, and is averaged over 10 different sets of patterns. We note that as each CAM neuron transitions from periodic to sparsely chaotic to densely chaotic states, the information retrieval capabilities are enhanced as evidenced by the reducing of the average Hamming distance, shown in Fig. 6 for $c = 4, 6$ (1-period and 2-period, respectively), $c = 8.5, 8.7$ (4-period and 8-period, respectively), $c = 9, 13$ (sparse chaos) and $c = 14$ (dense chaos). We note that the network exhibits the best performance for the sparse chaotic regimes. Table 1 lists the maximum Lyapunov exponents (Λ) for specific values of c in these cases.

TABLE I: The Maximum Lyapunov Exponents are tabulated for different values of parameter c

c	Λ
4	-0.000289
6	0.004151
8.5	0.008302
8.7	0.020135
9	0.035752
13	0.041952
14	0.084304

V. DISCUSSION

The CAM model proposed in this article is an oscillatory neural associative memory model that has the Rossler system as the fundamental unit or neuron. This provides us with a tool to quite naturally extend the current OAM models by leveraging the rich spectral properties of the Rossler system, and enables us to study it and comparing the effect of periodic and chaotic perturbations on the accurate retrieval pattern based on input stimulus for associative memory. As suggested in the articles by Nishikawa et al¹⁶ and Follman et al¹⁷, addition of periodic harmonic and multi-period harmonic perturbation helped increase the capacity of oscillator based associative memory models. We observe a further increase in the capacity by the addition of sparsely chaotic perturbation as noted in Fig 6 and greater precision in retrieval performance. We note a salient feature of the proposed model as compared to previous models^{16,17}, an independent control of the strength of the harmonics is not required, as it is implicit in the Rossler system. Additionally the hardware realisations of chaotic oscillators is an established field, and a hardware realisation of the proposed model is a future line of work that we are keen to pursue. If we allow for some error to persist in the retrieved pattern, our analysis yields a capacity of 0.08 per neuron for 30% initial error; for lesser introduced initial error the capacity can be noticeably increased, see Fig.6 and see Table- II for a comparison. Our model shows an increase in capacity similar to Hopfield networks with an increase in number of neurons, see Fig. 7a. The error bars represent the standard deviations to indicate how precise are the retrievals. As is expected, for lesser number of stored patterns ($p \leq 4$) the error is approximately zero, as the system converges completely to the desired patterns. Further, we note that as the number of stored patterns increase the average Hamming distance increases indicating the convergence is not entirely onto the desired patterns. .

Freeman and his coworkers, who performed extensive electrophysiological studies on the rabbit's olfactory bulb, had noticed that the spatiotemporal activities of the bulb are best described – not as a fixed point or a limit cycle oscillation – but as weak chaotic attractor (weakly chaotically modulated oscillations). When a set of odors were presented to the animal, even after the animal became familiar with a particular odor, repeated presentation of the odor resulted in

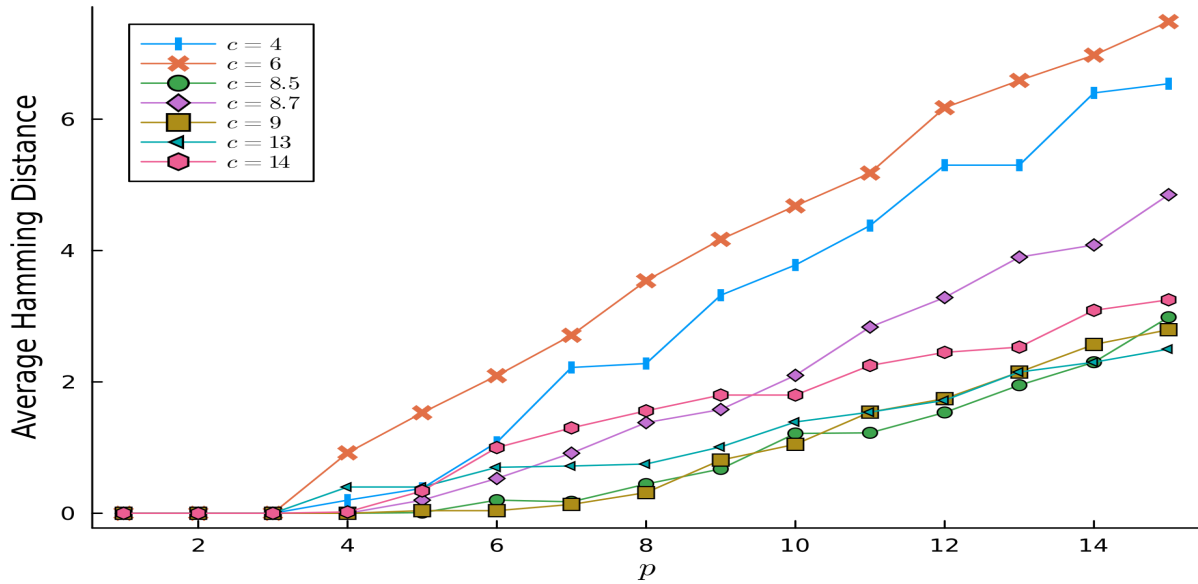


FIG. 6: Average Hamming distance plotted against number of patterns stored. The average Hamming distance is calculated based on Algorithm 1. The sparse chaotic regime shows the best performance.

TABLE II: Comparative Results of OAM

Model	Capacity	Comments
Nishikawa et al (2004)	0.04	Considered only perfect error free retrieval
Follmann et al (2015)	0.07	10% tolerance in the final retrieval
CAM,	0.08	6% tolerance in the final retrieval

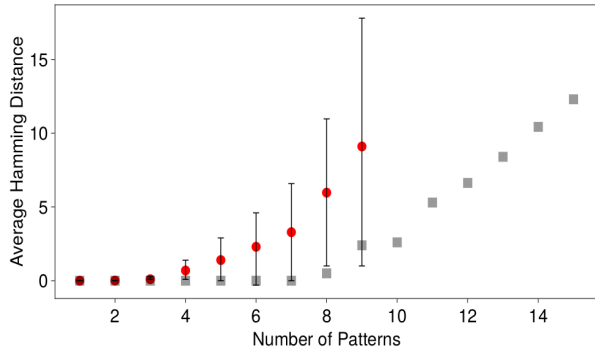
an “amplitude modulated” pattern that showed rich variability from trial to trial¹⁸. Our model is inspired by this hypothesis of Freeman and his coworkers that chaotic behaviour, rather than regular or random, constitutes as the ground state activity of the brain for sensory information processing, and serves as a means to ensure impartial and continual access to previously learned sensory patterns and as a mechanism to allow for novel sensory patterns to be learnt. In this brief we centralise our analysis around the former conception that the chaotic perturbations innate to the Rossler system’s phase dynamics allows for a more efficient oscillatory associative memory model. The chaotic pulses added to the phase dynamics ϕ by the z variable is comparable to the controlled source of noise, described in Sec III-B, that is suggested by them and allows for greater retrieval capabilities as reported in the previous section. Further, other biological ideas presented by Skarda and Freeman¹⁸ like the deep anaesthesia state can be witnessed in case of appropriate choice of the parameters (α, b, c) in which case the entire dynamics of the model approaches a point attractor, see Fig. 7b. Furthermore, as α varies from negative values to positive values, each Rossler

node undergoes bifurcation from fixed point attractor to limit cycle attractor. This can be compared to as the transition from anaesthetic state to wake state. However, the network in its present form doesn’t showcase the ability to utilise chaos to learn novel patterns, i.e. describe the transient dynamics when the system is initialised using novel patterns. This is a future line of study.

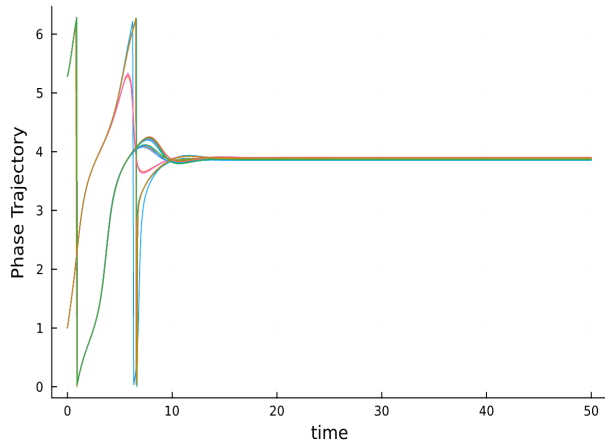
Additionally, recent results reported in^{29–33} are suggestive of that the healthy brain operates close to chaos, and “hovers” around this chaotic or critical state to effectively respond to environmental conditions. They describe this phenomenon using a critical branching process model wherein each node is a spiking neuron, and a neuron produces an activity on an average in σ other neurons, the average of which is defined as

$$\sigma = \frac{\text{number of descendants}}{\text{number of ancestors}}.$$

Here, ancestors of a neuron are the number of neurons that send an activation to it, while descendants are the number of neurons from which it receives activation. They show that when the expected branching parameter is tuned to 1, the information transmission, processing and storage is optimal. The network exhibits neuronal avalanches which show power law distributions, known as avalanche criticality. To see the effect of coupling strength, the Hamming distance is computed between the initial pattern fed to the model and the final retrieved pattern. For $\epsilon = 0.0$, the model is unable to perform any retrieval. As the coupling strength increases the systems ability to converge to the desired attractor increases, as the average Hamming distance reduces, however a minor increase in the error bars indicate that retrieval is not precise enough and the system tends to settle in some spurious attractors closer to the desired attractor. The retrieval ability peaks for $\epsilon \approx 0.0012$



(a) Average Hamming distance plotted against number of patterns stored. The average Hamming distances are calculated using Algorithm 1. The vertical error bars represent standard deviation. The CAM model shows an increase in model capacity and retrieval ability as the number of Rossler nodes increase. The parameters for the CAM model are $\alpha, \beta = 0.1, \epsilon = 13$ with coupling strength $\epsilon \approx 0.0012$.



(b) The trajectories of the individual CAM neurons approach a fixed point, for $(\alpha, \beta, \epsilon) = (-1.1, 0.1, 9)$

FIG. 7: The patterns are introduced with an initial 30% noise. As the system is allowed to evolve in time, the trajectories converge to a fixed point representing the deep anaesthetic state.

and the lower error bars indicate a greater precision in memory retrieval. A further increase in coupling strength causes an increase in average Hamming distance indicating poor retrieval ability. The increase in error bars further indicates that the system is unable to perform precise retrievals and converges to undesirable attractors; see Fig 8.

Further, we note that our model's retrieval performance increases as we transition to chaos; see Fig. 4D, marked by the third and fourth dashed lines. This is correlated with each Rossler node independently transitioning to chaos. Therefore, our models performance on storage capacity and retrieval performance is maximum at the edge of chaos, or atleast very close to it. Operation at edge of chaos has an interesting neurobiological significance. In experimental studies in neuroscience it has been observed that conscious-

ness is supported by edge of chaos, and evidence suggests that moving away from this critical point results in loss of consciousness.^{34,35} Similarly we observe that the models retrieval ability is lost as we move away from chaos. However, as reported by Karlis Kanders et al³⁶ that edge of chaos criticality scrutinised in this brief may not co-occur with the avalanche type criticality discussed in paragraph above, especially due to the complexity of each node in our network.

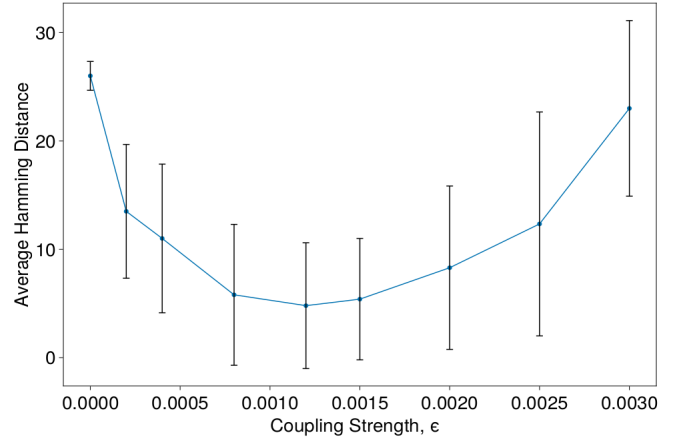


FIG. 8: The average Hamming distance varying with the coupling strength ϵ . The vertical error bars represent the standard deviation. The information retrieval peaks for coupling strength, $\epsilon = 0.0012$. The other parameters for the model are $\alpha, \beta = 0.1, \epsilon = 13$, and $p = 8$

There have been numerous networks that have leveraged the sensitive dependency of chaotic systems to improve performance on storing and retrieving abilities on associative memory models in the context of fixed point attractors.³⁷⁻⁴⁵ The addition of an analogue periodic mapping accompanied by the chaotic behaviour of the neuron aided the memory retrieval performances.^{37,38} A further increase in performance is reported by the addition of spatio-temporal chaos control^{42,43}. A Chaotic Neural Network possessing associative memory and pattern recognition capability was proposed by Adachi and his co-authors; a discrete four variable system with two/three internal states building upon the original Hopfield model utilizing the Ikeda map and delayed feedback to model Freeman's observations³⁹⁻⁴¹. Ke and Oommen showed that the Chaotic Neural Network by Adachi et al. (hereafter AdNN) shows a variety of different characteristics: associative memory, quasi-chaos and pattern recognition⁴⁶. Contrary to the Hopfield model where the system approaches a fixed state based on the input stimulus, in the AdNN the fixed patterns are approached periodically or quasi-chaotically. The same authors in a separate paper propose a variant of the chaotic neural network (LNN) based on the logistic map and simplifying the model to having only one additional internal state, retaining the associative memory and pattern recognition characteristics⁴⁷. However one drawback is that the model has only negative Lyapunov exponents but preserves

high aperiodicity observed in AdNN. Our model is particularly advantageous in the sense it shows chaotic behaviour as evidenced by Table I and Fig.4(D), and as established in Sec-III B, is imperative to increase the retrieval performance capability as the number of patterns stored increases; and gives greater insight into the importance of chaotic activity in terms of spectral analysis. However, the inability to show long term transient dynamics corresponding to an "unknown" state when the system is exposed to a novel pattern, as is described by AdNN and LNN, is a potential limitation of our model in its present form.

VI. CONCLUDING REMARKS

In this article we proposed a Chaotic Neural Associative Memory oscillator model based on the chaotic dynamics of Rossler system aligning with the hypothesis proposed by Freeman and his associates: Brain relies on chaotic rather than regular or random/noisy activity for sensory perception. The proposed CAM model achieves state of the art performance for oscillator based associative memory models yielding a capacity of 0.08 patterns per neuron with almost perfect retrieval for patterns with up to 30% of distorted bits in the initial stimuli. Our model relies on weakly chaotic perturbations to the phase dynamics to increase its performance capability; provoking the idea that chaotic activity of a neuron ensemble is quite possibly fundamental to the efficient information processing in the brain.

ACKNOWLEDGMENTS

This work was financially supported by CSIR. We deeply appreciate the contributions by IIT Madras. The authors would like to acknowledge the partial funding received from the Ministry of Education, Govt of India towards Institute of Eminence, funds for Complex Systems and Dynamics, project no. SP2021077 DRMHRD/DIRIIT.

DATA AVAILABILITY STATEMENT

Data sharing is not applicable to this article as no new data were created or analyzed in this study.

CONFLICT OF INTEREST STATEMENT

The authors have no conflicts to disclose.

REFERENCES

- ¹D. J. Amit and A. Treves, "Associative memory neural network with low temporal spiking rates." *Proceedings of the National Academy of Sciences* **86**, 7871–7875 (1989), <https://www.pnas.org/doi/pdf/10.1073/pnas.86.20.7871>.
- ²J. J. Hopfield, "Neural networks and physical systems with emergent collective computational abilities." *Proceedings of the National Academy of Sciences* **79**, 2554–2558 (1982), <https://www.pnas.org/doi/pdf/10.1073/pnas.79.8.2554>.
- ³J. J. Hopfield, "Neurons with graded response have collective computational properties like those of two-state neurons." *Proceedings of the National Academy of Sciences* **81**, 3088–3092 (1984), <https://www.pnas.org/doi/pdf/10.1073/pnas.81.10.3088>.
- ⁴B. Kosko, "Bidirectional associative memories," *IEEE Transactions on Systems, Man, and Cybernetics* **18**, 49–60 (1988).
- ⁵D. H. Ackley, G. E. Hinton, and T. J. Sejnowski, "A learning algorithm for boltzmann machines," *Cognitive Science* **9**, 147–169 (1985).
- ⁶M. A. Cohen and S. Grossberg, "Absolute stability of global pattern formation and parallel memory storage by competitive neural networks," *IEEE transactions on systems, man, and cybernetics* , 815–826 (1983).
- ⁷J. Fell, P. Klaver, K. Lehnertz, T. Grunwald, C. Schaller, C. E. Elger, and G. Fernández, "Human memory formation is accompanied by rhinal-hippocampal coupling and decoupling," *Nature neuroscience* **4**, 1259–1264 (2001).
- ⁸E. Düzel, W. D. Penny, and N. Burgess, "Brain oscillations and memory," *Current opinion in neurobiology* **20**, 143–149 (2010).
- ⁹J. O'Keefe and M. L. Recce, "Phase relationship between hippocampal place units and the eeg theta rhythm," *Hippocampus* **3**, 317–330 (1993), <https://onlinelibrary.wiley.com/doi/pdf/10.1002/hipo.450030307>.
- ¹⁰M. Siegel, M. R. Warden, and E. K. Miller, "Phase-dependent neuronal coding of objects in short-term memory," *Proceedings of the National Academy of Sciences* **106**, 21341–21346 (2009).
- ¹¹L. Abbott, "A network of oscillators," *Journal of Physics A: Mathematical and General* **23**, 3835 (1990).
- ¹²S. V. Chakravarthy and J. Ghosh, "A complex-valued associative memory for storing patterns as oscillatory states," *Biological Cybernetics* **75**, 229–238 (1996).
- ¹³F. C. Hoppensteadt and E. M. Izhikevich, "Pattern recognition via synchronization in phase-locked loop neural networks," *IEEE Transactions on Neural Networks* **11**, 734–738 (2000).
- ¹⁴F. C. Hoppensteadt and E. M. Izhikevich, "Synchronization of mems resonators and mechanical neurocomputing," *IEEE Transactions on Circuits and Systems I: Fundamental Theory and Applications* **48**, 133–138 (2001).
- ¹⁵T. Aonishi, "Phase transitions of an oscillator neural network with a standard hebb learning rule," *Phys. Rev. E* **58**, 4865–4871 (1998).
- ¹⁶T. Nishikawa, F. C. Hoppensteadt, and Y.-C. Lai, "Oscillatory associative memory network with perfect retrieval," *Physica D: Nonlinear Phenomena* **197**, 134–148 (2004).
- ¹⁷R. Follmann, E. E. N. Macau, E. Rosa, and J. R. C. Piqueira, "Phase oscillator network and visual pattern recognition," *IEEE Transactions on Neural Networks and Learning Systems* **26**, 1539–1544 (2015).
- ¹⁸C. A. Skarda and W. J. Freeman, "How brains make chaos in order to make sense of the world," *Behavioral and Brain Sciences* **10**, 161–173 (1987).
- ¹⁹J. D. c. Farmer, "spectral broadening of period-doubling bifurcation sequences," *Phys. Rev. Lett.* **47**, 179–182 (1981).
- ²⁰M. G. Rosenblum, A. S. Pikovsky, and J. Kurths, "Phase synchronization of chaotic oscillators," *Phys. Rev. Lett.* **76**, 1804–1807 (1996).
- ²¹A. S. Pikovsky, M. G. Rosenblum, G. V. Osipov, and J. Kurths, "Phase synchronization of chaotic oscillators by external driving," *Physica D: Nonlinear Phenomena* **104**, 219–238 (1997).
- ²²J. D. Farmer, "Spectral broadening of period-doubling bifurcation sequences," *Phys. Rev. Lett.* **47**, 179–182 (1981).
- ²³J. Bezanson, A. Edelman, S. Karpinski, and V. B. Shah, "Julia: A fresh approach to numerical computing," *SIAM Review* **59**, 65–98 (2017).
- ²⁴C. Rackauckas and Q. Nie, "Differentials.jl—a performant and feature-rich ecosystem for solving differential equations in julia," *Journal of Open Research Software* **5**, 15 (2017).
- ²⁵Y. Ma, S. Gowda, R. Anantharaman, C. Laughman, V. Shah, and C. Rackauckas, "Modelingtoolkit: A composable graph transformation system for equation-based modeling," (2021), [arXiv:2103.05244 \[cs.MS\]](https://arxiv.org/abs/2103.05244).
- ²⁶D. J. Gardner, D. R. Reynolds, C. S. Woodward, and C. J. Balos, "Enabling new flexibility in the SUNDIALS suite of nonlinear and differential/algebraic equation solvers," *ACM Transactions on Mathematical Software (TOMS)* (2022), 10.1145/3539801.

- ²⁷A. C. Hindmarsh, P. N. Brown, K. E. Grant, S. L. Lee, R. Serban, D. E. Shumaker, and C. S. Woodward, "SUNDIALS: Suite of nonlinear and differential/algebraic equation solvers," *ACM Transactions on Mathematical Software (TOMS)* **31**, 363–396 (2005).
- ²⁸L. Deng, "The mnist database of handwritten digit images for machine learning research," *IEEE Signal Processing Magazine* **29**, 141–142 (2012).
- ²⁹N. Friedman, S. Ito, B. A. W. Brinkman, M. Shimono, R. E. L. DeVillie, K. A. Dahmen, J. M. Beggs, and T. C. Butler, "Universal critical dynamics in high resolution neuronal avalanche data," *Phys. Rev. Lett.* **108**, 208102 (2012).
- ³⁰M. G. Kitzbichler, M. L. Smith, S. R. Christensen, and E. Bullmore, "Broadband criticality of human brain network synchronization," *PLOS Computational Biology* **5**, 1–13 (2009).
- ³¹V. Zimmer, "Why brain criticality is clinically relevant: A scoping review," *Frontiers in Neural Circuits* **14** (2020), 10.3389/fncir.2020.00054.
- ³²L. J. Fosque, R. V. Williams-García, J. M. Beggs, and G. Ortiz, "Evidence for quasycritical brain dynamics," *Phys. Rev. Lett.* **126**, 098101 (2021).
- ³³J. M. Beggs, "The criticality hypothesis: how local cortical networks might optimize information processing," *Philosophical Transactions of the Royal Society A: Mathematical, Physical and Engineering Sciences* **366**, 329–343 (2008), <https://royalsocietypublishing.org/doi/pdf/10.1098/rsta.2007.2092>.
- ³⁴D. Toker, I. Pappas, J. D. Lendner, J. Frohlich, D. M. Mateos, S. Muthukumaraswamy, R. Carhart-Harris, M. Paff, P. M. Vespa, M. M. Monti, F. T. Sommer, R. T. Knight, and M. D'Esposito, "Consciousness is supported by near-critical slow cortical electrodynamics," *Proceedings of the National Academy of Sciences* **119**, e2024455119 (2022), <https://www.pnas.org/doi/pdf/10.1073/pnas.2024455119>.
- ³⁵L. Cocchi, L. L. Gollo, A. Zalesky, and M. Breakspear, "Criticality in the brain: A synthesis of neurobiology, models and cognition," *Progress in neurobiology* **158**, 132–152 (2017).
- ³⁶K. Kandera, T. Lorimer, and R. Stoop, "Avalanche and edge-of-chaos criticality do not necessarily co-occur in neural networks," *Chaos: An Interdisciplinary Journal of Nonlinear Science* **27**, 047408 (2017), https://pubs.aip.org/aip/cha/article-pdf/doi/10.1063/1.4978998/13299098/047408_1_online.pdf.
- ³⁷M. Nakagawa, "chaos synergetic neural network," *Journal of the Physical Society of Japan* **64**, 3112–3119 (1995), <https://doi.org/10.1143/JPSJ.64.3112>.
- ³⁸M. Nakagawa, "chaos associative memory model," in *Proceedings of the IEEE International Symposium on Intelligent Control* (2002) pp. 508–513.
- ³⁹M. Adachi and K. Aihara, "Associative dynamics in a chaotic neural network," *Neural Networks* **10**, 83–98 (1997).
- ⁴⁰K. Aihara, T. Takabe, and M. Toyoda, "Chaotic neural networks," *Physics letters A* **144**, 333–340 (1990).
- ⁴¹D. Calitoui, B. J. Oommen, and D. Nussbaum, "Desynchronizing a chaotic pattern recognition neural network to model inaccurate perception," *IEEE Transactions on Systems, Man, and Cybernetics, Part B (Cybernetics)* **37**, 692–704 (2007).
- ⁴²Guoguang He, L. Chen, and K. A. , "associative memory with a controlled chaotic neural network," *Neurocomputing* **71**, 2794–2805 (2008), artificial Neural Networks (ICANN 2006) / Engineering of Intelligent Systems (ICEIS 2006).
- ⁴³M. Kushibe, Y. Liu, and J. c. Ohtsubo, "associative memory with spatiotemporal chaos control," *Phys. Rev. E* **53**, 4502–4508 (1996).
- ⁴⁴J. Kitada, Y. Osana, and E. c. Hagiwara, "chaotic episodic associative memory," in *SMC'98 Conference Proceedings. 1998 IEEE International Conference on Systems, Man, and Cybernetics (Cat. No.98CH36218)*, Vol. 4 (1998) pp. 3629–3634 vol.4.
- ⁴⁵I. Tsuda, "dynamic link of memory—chaotic memory map in nonequilibrium neural networks," *Neural networks* **5**, 313–326 (1992).
- ⁴⁶K. Qin and B. J. Oommen, "Chaotic pattern recognition: The spectrum of properties of the adachi neural network," in *Structural, Syntactic, and Statistical Pattern Recognition: Joint IAPR International Workshop, SSPR & SPR 2008, Orlando, USA, December 4-6, 2008. Proceedings* (Springer, 2008) pp. 540–550.
- ⁴⁷Q. Ke and B. J. Oommen, "Logistic neural networks: Their chaotic and pattern recognition properties," *Neurocomputing* **125**, 184–194 (2014), advances in Neural Network Research and Applications Advances in Bio-Inspired Computing: Techniques and Applications.